Validation of sea ice concentration observations in the Fram Strait marginal ice zone during May 2017

Z. Labe[1]

[1]Department of Earth System Science, University of California, Irvine, California, USA

Key Points:

- Sea ice cover varies at the edge of the Fram Strait marginal ice zone with significant day-to-day fluctuations
- AMSR2 ASI-3k (3.125 km) captures the sea ice edge, but is unable to resolve the smaller leads and sea ice dispersion during the duration of the R/V *Lance* field cruise
- In situ and remote sensing observations need standardized methods for comparisons and verification

Corresponding author: Zachary Labe, zlabe@uci.edu

Abstract

The continuous passive microwave satellite record of Arctic sea ice is a critical data set to understanding Arctic climate variability and change. Numerous satellite and reanalysis data sets provide sea ice concentration measurements, but further validation is needed to assess their biases and uncertainties. Here we evaluate high resolution sea ice concentration observations from the 3.125 km (ASI-3k) Advanced Microwave Scanning Radiometer 2 (AMSR2) product to compare with ground observations during a field cruise in the Fram Strait from 18-24th May 2017. ASI-3k closely resolves the marginal sea ice zone edge and larger leads, but overestimates in areas of more dispersed sea ice. Further improvements to the spatial resolution of sea ice satellite observations will assist scientists and numerous stakeholders in documenting future Arctic sea ice loss

1 Introduction

The Arctic has witnessed significant changes in sea ice extent (SIE) [*Serreze et al.*, 2007] and thickness (SIT) [*Kwok and Rothrock*, 2009], surface temperature warming [*Screen and Simmonds*, 2010], and changes in the large-scale atmospheric circulation [*Overland et al.*, 2012; *Cohen et al.*, 2014] during the last several decades. However, large uncertainties remain in remote sensing observations of sea ice [*Zygmuntowska et al.*, 2014; *Ivanova et al.*, 2015], reanalysis data sets [*Lindsay et al.*, 2014], and future climate model projections [*Stroeve et al.*, 2012; *Rosenblum et al.*, 2017]. Improving the amount of in situ observations in the Arctic is important for analyzing long-term sea ice and climate variability. Further, in situ observations provide ground validation tests to resolve climate data set uncertainties and biases.

Arctic field cruises have been previously used for validating sea ice concentration (SIC) [e.g., *Spreen et al.*, 2008] and SIT [e.g., *Kaleschke et al.*, 2016] with remote sensing observations. This paper evaluates SIC observations between ship observations from a mid-May field cruise (R/V *Lance*) in the marginal ice zone northwest of Svalbard ($\approx 80°$N latitude). While the passive microwave satellite record provides one of the longest data sets documenting Arctic sea ice [*Parkinson et al.*, 1999], there remain uncertainties in various products due to cloud cover, atmospheric absorption and emissivity, surface roughness, and snow surface properties [*Rayner et al.*, 2003; *Andersen et al.*, 2007]. While this analysis is limited in space and time (as a result of the field cruise), we provide an assessment of in situ SIC observations with the new high-resolution (3.125 km) Advanced

Microwave Scanning Radiometer 2 (AMSR2) SIC product (ASI-3k) provided by the University of Hamburg [*Beitsch et al.*, 2014].

Here we assess the differences between observed SIC on the R/V *Lance* field cruise with the high resolution ASI-3k product over the 18-24 May 2017 period. In section 2 we discuss the sea ice data sets and methods of analysis. Section 3 examines the changes and differences in sea ice cover during the field cruise. Finally, section 4 discusses uncertainties in observations and the need for continued high temporal and spatial remote sensing of the Arctic.

2 Data and Methods

2.1 R/V *Lance*

Sea ice observations were taken following the Arctic Shipborne Sea Ice Standardization Tool (ASSIST) developed by Climate and Cryosphere (CliC) Arctic Sea Ice Working Group (ASIWG) in August 2012 [*Orlich et al.*, 2013]. The ASSIST software is freely available at `http://www.iarc.uaf.edu/icewatch` along with open-access data of near-real time sea ice observations from participating vessels. The observations follow the (1970) World Meteorological Organization (WMO) nomenclature and the Antarctic Sea Ice and Processes & Climate (ASPeCt) protocol [*Orlich et al.*, 2013]. Observable parameters in the ASSIST software include: weather conditions, SIC, sea ice age, snow type and depth, algae and sediment accumulation, sea ice topography and ice ridges, melt ponds, and open water fraction.

Observations during the R/V *Lance* field cruise were taken hourly while maneuvering through the marginal ice zone and every 3-hours while anchored/drifting with sea ice floes (19-23 May 2017). However, there are inconsistencies in these observations as a result of different observers (more than 10 people) and missed observation times. Photographs were also taken at every observation period facing port, starboard, and forward in the ship bridge. Visibility also restricted the view during observations from fog, blowing snow, and occasional snow squalls. Finally, biases may also exist as the R/V *Lance* is not an icebreaker, and therefore, it particularly travels through lead openings and areas of thinner ice. SIC values are reported in tenths (0-10). While large uncertainties arise from the bridge observers' reports, they are particularly useful given the lack of ground obser-

vations in the Arctic and have been used for validation in prior studies [e.g., *Spreen et al.*, 2008].

2.2 Sea ice data

We use daily SIE in the Greenland Sea from the National Snow and Ice Data Center (NSIDC) Arctic Sea Ice Index, version 2 [*Fetterer et al.*, 2017]. SIE is derived from grid cells averaging at least 15% in SIC and uses the NASA Team methods by *Cavalieri et al.* [1984]. The passive microwave satellite record of SIC is derived from brightness temperature extending from 1978 through the present.

For comparison with ground observations from the R/V *Lance*, we use the new Advanced Microwave Scanning Radiometer 2 (AMSR2) data set of SIC [*Beitsch et al.*, 2014] using the ARTIST Sea Ice algorithm [*Spreen et al.*, 2008] on a 3.125 x 3.125 km polar stereographic grid (ASI-3k). Daily data is available from 1 August 2012. SIC is derived from polarization differences in brightness temperature on the AMSR2 89 GHz channel. Estimates by *Spreen et al.* [2008] found the ARTIST algorithm for SIC correlated 0.8 with ship observations, and the largest differences were found near areas of thin ice (especially < 20 cm) [*Kern et al.*, 2003; *Scott et al.*, 2015]. Additionally, *Beitsch et al.* [2014] showed close agreement between MODIS imagery and ASI-3k SIC in their analysis of a large fracture event (2013) in the Beaufort Sea. ASI-3k provides the highest resolution data set of global SIC.

2.3 Methods

We assess the seasonal cycle of SIE in the Greenland Sea from 1978 to 2017. The Greenland Sea is defined by the NSIDC regional mask in *Parkinson et al.* [1999] from southern Greenland to (and including) Svalbard. The mean SIE is defined by a 1981 to 2010 climatology. We focus on the SIE during the period of the field cruise from 18-23 May 2017.

SIC from ASI-3k were rounded to the nearest tenth for consistency with the R/V *Lance* observations. A time series was created of ASI-3k SIC from 19-23 May 2017 for a region of the Fram Strait (Greenland Sea) just northwest of Svalbard. Additionally, a composite of ASI-3k SIC in this spatial domain was averaged over the time period. Compar-

isons between satellite and observational SIC were made for each day and with the time series composite average.

3 Results

Fig. 1 shows SIE in the Greenland Sea from November 1978 to June 2017. January 2017 SIE was the lowest on record in the Greenland, but has since risen closer to average during spring. SIE during the field cruise was near the 1981-2010 climatological average with May 2017 ranking 19th (out of 39) for lowest SIE. Similarly, sea ice area (SIA) was near average and ranked 23rd (not shown). Overall, there is a decline of SIE in all months during the satellite era in the Greenland Sea. This is especially found in the winter and spring. Analysis by *Smedsrud et al.* [2017] show significant interannual variability of sea ice export in the Fram Strait, but also a loss of September SIE since the mid-1970s.

The track of the R/V *Lance* is shown in Fig. 2 along with the ship's SIC observations and mean composite of ASI-3k SIC (19-23 May 2017). In contrast to ASI-3k, no sea ice was observed along the west coast of Svalbard and near Prins Karls Forland. The marginal sea ice zone edge is well captured by ASI-3k and consistent with ship observations. Fig. 3 highlights SIC observations from the R/V *Lance* and shows a well defined ice edge with SIC increasing from 10% to 70% in a 3-hour period entering the marginal ice zone (May 19th). Similarly, this is found leaving the ice pack on the 23rd. SIC varied between 70% and 90% while in the marginal ice zone and anchored to ice floes, although this may be biased by the R/V *Lance* traveling through lead openings and thinner ice areas. The R/V *Lance* anchored to several ice floes and drifted with the sea ice during these periods. The frequency of SIC observations were reduced to every 3-hours, but variability was still found in the fraction of open water and lead size.

Finally, Fig. 4 analyzes each day of the field cruise for a comparison between in situ ship SIC observations and ASI-3k. Entering the sea ice pack on May 19th shows a sharp edge to the marginal ice zone with in situ observations comparing closely to ASI-3k. The best agreement between these two observation data sets is during this period. On May 20th the R/V *Lance* primarily remained anchored and drifted with a sea ice floe. Ship observations were between approximately 70-80% SIC while ASI-3k showed complete ice cover (100%). These differences may result from the 3.125 km resolution in ASI-3k, which is unable to resolve smaller leads and higher uncertainty in areas of thinner

ice [*Scott et al.*, 2015]. Likewise, these discrepancies are also found on May 21st. ASI-3k shows the marginal ice zone slightly retreated starting on May 22nd and became more dispersed. Comparisons between ship observations and ASI-3k, however, show fairly close agreement despite increasing sea ice dispersion. The ASI-3k is only available once per day, and therefore would not be expected to account for ongoing abrupt changes in sea ice shape and motion.

4 Summary and conclusions

The Arctic has undergone dramatic changes over the last several decades [e.g., *Serreze et al.*, 2009; *Stroeve et al.*, 2011; *Laxon et al.*, 2013; *Cohen et al.*, 2014] and in particular for areas close to Svalbard [e.g., *Nordli et al.*, 2014; *Isaksen et al.*, 2016; *Descamps et al.*, 2017]. Here we evaluated the high resolution ASI-3k satellite SIC product with in situ observations during a field cruise (R/V *Lance*) in the Fram Strait just northwest of Svalbard (18-24 May 2017). ASI-3k compares well with the ship SIC observations, particularly at the edge of the marginal ice zone. However, in the sea ice pack, we find differences between the two data sets with the ship observations approximately 20-30% less than ASI-3k. We note that there may be additional uncertainties from the ship observations as a result of different observers, restricted visibility from blowing snow and weather, changes in the frequency of observations, and influence of the R/V *Lance* track.

The recent Norwegian Young Sea Ice Cruise (N-ICE2015) field campaign by the R/V *Lance* demonstrated the importance of collecting and verifying ground observations in a changing Arctic [e.g., *Granskog et al.*, 2016; *Graham et al.*, 2017]. To improve our understanding of long-term Arctic climate variability, more in situ observations are needed for comparison with passive microwave satellite products. Uncertainties still remain between these different sea ice data sets and algorithms, which can affect climate models and reanalysis [*Bunzel et al.*, 2016; *Ivanova et al.*, 2015]. While a larger spatial domain and longer temporal range of observations is needed, our assessment shows close agreement between in situ observations and the ASI-3k satellite product of SIC during the field cruise.

Acknowledgments

This report is in part of a 3-year INTPART project: “Arctic Field Summer Schools: Norway-Canada-USA collaboration” (NFR project 261786/H30). The R/V *Lance* was chartered

from 18-24 May 2017 out of Longyearbyen, Svalbard. We thank the captain and crew for their assistance on board. Python 2.7 was used for data processing and plotting. All code used for this manuscript is available in an online repository at `https://github.com/zmlabe/INTPART`. AMSR2 ASI-3k satellite data is freely available from `ftp://ftp-projects.zmaw.de/seaice/AMSR2/`. Sea ice extent data can be downloaded from the National Snow and Ice Data Center at `http://nsidc.org/data/docs/noaa/g02135_seaice_index/`. Any additional data may be available upon request from Z. Labe.

References

Andersen, S., R. Tonboe, L. Kaleschke, G. Heygster, and L. T. Pedersen (2007), Intercomparison of passive microwave sea ice concentration retrievals over the high-concentration Arctic sea ice, *Journal of Geophysical Research*, *112*(C8), C08,004, doi:10.1029/2006JC003543.

Beitsch, A., L. Kaleschke, and S. Kern (2014), Investigating High-Resolution AMSR2 Sea Ice Concentrations during the February 2013 Fracture Event in the Beaufort Sea, *Remote Sensing*, *6*(5), 3841–3856, doi:10.3390/rs6053841.

Bunzel, F., D. Notz, J. Baehr, W. A. Muller, and K. Frohlich (2016), Seasonal climate forecasts significantly affected by observational uncertainty of Arctic sea ice concentration, *Geophysical Research Letters*, *43*(2), 852–859, doi:10.1002/2015GL066928.

Cavalieri, D. J., P. Gloersen, and W. J. Campbell (1984), Determination of sea ice parameters with the NIMBUS 7 SMMR, *Journal of Geophysical Research: Atmospheres*, *89*(D4), 5355–5369, doi:10.1029/JD089iD04p05355.

Cohen, J., J. A. Screen, J. C. Furtado, M. Barlow, D. Whittleston, D. Coumou, J. Francis, K. Dethloff, D. Entekhabi, J. Overland, and J. Jones (2014), Recent Arctic amplification and extreme mid-latitude weather, *Nature Geoscience*, *7*(9), 627–637, doi:10.1038/ngeo2234.

Descamps, S., J. Aars, E. Fuglei, K. M. Kovacs, C. Lydersen, O. Pavlova, A. O. Pedersen, V. Ravolainen, and H. Strom (2017), Climate change impacts on wildlife in a High Arctic archipelago - Svalbard, Norway, *Global Change Biology*, *23*(2), 490–502, doi:10.1111/gcb.13381.

Fetterer, F., K. K, W. Meier, and M. Savoie (2017), Sea Ice Index, Version 2, doi:http://dx.doi.org/10.7265/N5736NV7.

Graham, R. M., A. Rinke, L. Cohen, S. R. Hudson, V. P. Walden, M. A. Granskog, W. Dorn, M. Kayser, and M. Maturilli (2017), A comparison of the two Arctic atmospheric winter states observed during N-ICE2015 and SHEBA, *Journal of Geophysical Research: Atmospheres*, *122*(11), 5716–5737, doi:10.1002/2016JD025475.

Granskog, M., P. Assmy, S. Gerland, G. Spreen, H. Steen, and L. Smedsrud (2016), Arctic Research on Thin Ice: Consequences of Arctic Sea Ice Loss, *Eos*, *97*, doi:10.1029/2016EO044097.

Isaksen, K., O. Nordli, E. J. Forland, E. Lupikasza, S. Eastwood, and T. Niedzwiedz (2016), Recent warming on Spitsbergen-Influence of atmospheric circulation and sea

ice cover, *Journal of Geophysical Research: Atmospheres*, *121*(20), 11,913–11,931, doi: 10.1002/2016JD025606.

Ivanova, N., L. T. Pedersen, R. T. Tonboe, S. Kern, G. Heygster, T. Lavergne, A. Sørensen, R. Saldo, G. Dybkjær, L. Brucker, and M. Shokr (2015), Inter-comparison and evaluation of sea ice algorithms: towards further identification of challenges and optimal approach using passive microwave observations, *The Cryosphere*, *9*(5), 1797–1817, doi: 10.5194/tc-9-1797-2015.

Kaleschke, L., X. Tian-Kunze, N. Maaß, A. Beitsch, A. Wernecke, M. Miernecki, G. Müller, B. H. Fock, A. M. Gierisch, K. H. Schlünzen, T. Pohlmann, M. Dobrynin, S. Hendricks, J. Asseng, R. Gerdes, P. Jochmann, N. Reimer, J. Holfort, C. Melsheimer, G. Heygster, G. Spreen, S. Gerland, J. King, N. Skou, S. S. Søbjærg, C. Haas, F. Richter, and T. Casal (2016), SMOS sea ice product: Operational application and validation in the Barents Sea marginal ice zone, *Remote Sensing of Environment*, *180*, 264–273, doi:10.1016/j.rse.2016.03.009.

Kern, S., L. Kaleschke, and D. Clausi (2003), A Comparison of Two 85-GHz SSM/I Ice Concentration Algorithms With AVHRR and ERS-2 SAR Imagery, *IEEE Transactions on Geoscience and Remote Sensing*, *41*(10), 2294–2306, doi:10.1109/TGRS.2003.817181.

Kwok, R., and D. A. Rothrock (2009), Decline in Arctic sea ice thickness from submarine and ICESat records: 1958-2008, *Geophysical Research Letters*, *36*(15), n/a–n/a, doi: 10.1029/2009GL039035.

Laxon, S. W., K. A. Giles, A. L. Ridout, D. J. Wingham, R. Willatt, R. Cullen, R. Kwok, A. Schweiger, J. Zhang, C. Haas, S. Hendricks, R. Krishfield, N. Kurtz, S. Farrell, and M. Davidson (2013), CryoSat-2 estimates of Arctic sea ice thickness and volume, *Geophysical Research Letters*, *40*(4), 732–737, doi:10.1002/grl.50193.

Lindsay, R., M. Wensnahan, A. Schweiger, J. Zhang, R. Lindsay, M. Wensnahan, A. Schweiger, and J. Zhang (2014), Evaluation of Seven Different Atmospheric Reanalysis Products in the Arctic*, *http://dx.doi.org/10.1175/JCLI-D-13-00014.1*.

Nordli, O., R. Przybylak, A. E. Ogilvie, and K. Isaksen (2014), Long-term temperature trends and variability on Spitsbergen: the extended Svalbard Airport temperature series, 1898?2012, *Polar Research*, *33*(1), 21,349, doi:10.3402/polar.v33.21349.

Orlich, A., J. K. Hutchings, and T. M. Green (2013), Observing Arctic Sea Ice from Bow to Screen: Introducing Ice Watch, the Data Network of Near Real-Time and Historic

239 Observations from the Arctic Shipborne Sea Ice Standardization Tool (ASSIST), *Ameri-*
240 *can Geophysical Union, Fall Meeting 2013, abstract #C31B-0652*.

241 Overland, J. E., J. A. Francis, E. Hanna, and M. Wang (2012), The recent shift in early
242 summer Arctic atmospheric circulation, *Geophysical Research Letters*, *39*(19), n/a–n/a,
243 doi:10.1029/2012GL053268.

244 Parkinson, C. L., D. J. Cavalieri, P. Gloersen, H. J. Zwally, and J. C. Comiso (1999),
245 Arctic sea ice extents, areas, and trends, 1978-1996, *Journal of Geophysical Research:*
246 *Oceans*, *104*(C9), 20,837–20,856, doi:10.1029/1999JC900082.

247 Rayner, N. A., D. E. Parker, E. B. Horton, C. K. Folland, L. V. Alexander, D. P. Rowell,
248 E. C. Kent, and A. Kaplan (2003), Global analyses of sea surface temperature, sea ice,
249 and night marine air temperature since the late nineteenth century, *Journal of Geophysi-*
250 *cal Research*, *108*(D14), 4407, doi:10.1029/2002JD002670.

251 Rosenblum, E., I. Eisenman, E. Rosenblum, and I. Eisenman (2017), Sea ice trends in
252 climate models only accurate in runs with biased global warming, *Journal of Climate*,
253 pp. JCLI–D–16–0455.1, doi:10.1175/JCLI-D-16-0455.1.

254 Scott, K. A., Z. Ashouri, M. Buehner, L. Pogson, and T. Carrieres (2015), Assimila-
255 tion of ice and water observations from SAR imagery to improve estimates of sea ice
256 concentration, *Tellus A: Dynamic Meteorology and Oceanography*, *67*(1), 27,218, doi:
257 10.3402/tellusa.v67.27218.

258 Screen, J. A., and I. Simmonds (2010), The central role of diminishing sea ice in recent
259 Arctic temperature amplification., *Nature*, *464*(7293), 1334–7, doi:10.1038/nature09051.

260 Serreze, M. C., M. M. Holland, and J. Stroeve (2007), Perspectives on the Arctic's Shrink-
261 ing Sea-Ice Cover, *Science*, *315*(5818).

262 Serreze, M. C., A. P. Barrett, J. C. Stroeve, D. N. Kindig, and M. M. Holland (2009), The
263 emergence of surface-based Arctic amplification, *The Cryosphere*, *3*(1), 11–19, doi:10.
264 5194/tc-3-11-2009.

265 Smedsrud, L. H., M. H. Halvorsen, J. C. Stroeve, R. Zhang, and K. Kloster (2017), Fram
266 Strait sea ice export variability and September Arctic sea ice extent over the last 80
267 years, *The Cryosphere*, *11*(1), 65–79, doi:10.5194/tc-11-65-2017.

268 Spreen, G., L. Kaleschke, and G. Heygster (2008), Sea ice remote sensing using AMSR-
269 E 89-GHz channels, *Journal of Geophysical Research*, *113*(C2), C02S03, doi:10.1029/
270 2005JC003384.

Stroeve, J. C., M. C. Serreze, M. M. Holland, J. E. Kay, J. Malanik, and A. P. Barrett (2011), The Arctic's rapidly shrinking sea ice cover: a research synthesis, *Climatic Change*, *110*(3-4), 1005–1027, doi:10.1007/s10584-011-0101-1.

Stroeve, J. C., V. Kattsov, A. Barrett, M. Serreze, T. Pavlova, M. Holland, and W. N. Meier (2012), Trends in Arctic sea ice extent from CMIP5, CMIP3 and observations, *Geophysical Research Letters*, *39*(16), n/a–n/a, doi:10.1029/2012GL052676.

Zygmuntowska, M., P. Rampal, N. Ivanova, and L. H. Smedsrud (2014), Uncertainties in Arctic sea ice thickness and volume: new estimates and implications for trends, *The Cryosphere*, *8*(2), 705–720, doi:10.5194/tc-8-705-2014.

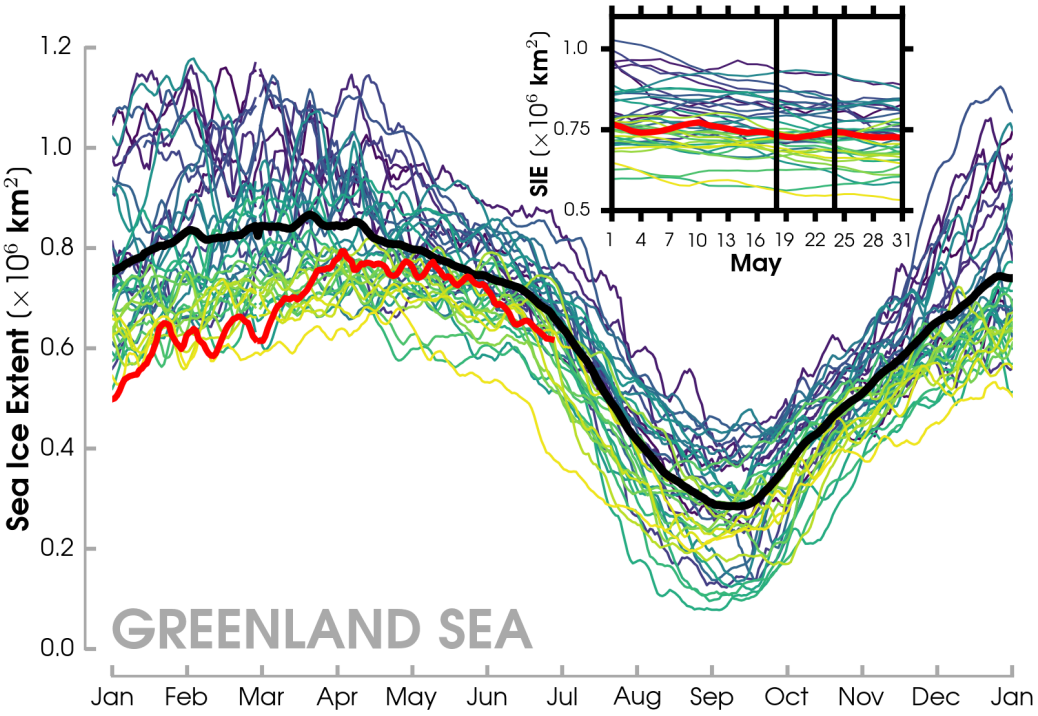

Figure 1. Seasonal cycle of daily sea ice extent (SIE) in the Greenland Sea from 1978 to 2017. The (line) color gradient shows older (purple) to more recent years (yellow). 2017 is shown in red, and the 1981 to 2010 mean is in black. The subplot indicates SIE during May with vertical lines highlighting the period of the R/V *Lance* cruise. SIE is computed from sea ice concentration with grid cells of at least 15% coverage.

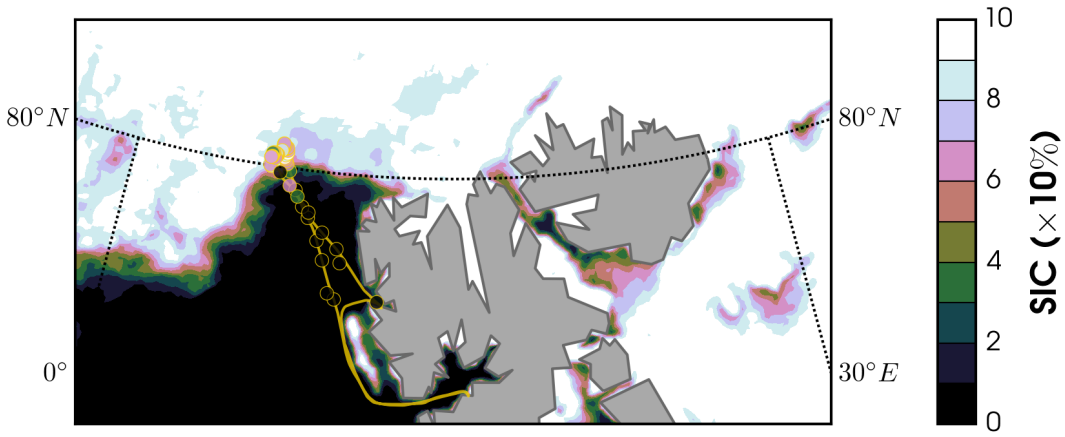

Figure 2. Sea ice concentration (SIC) measured from personal observations during the R/V *Lance* field cruise (19-23 May 2017) shown by scatter points. The ship track is indicated by the yellow line (northwest of Svalbard). Color gradient of filled contours show SIC from AMSR2 ASI-3k averaged over 19 to 23 May 2017.

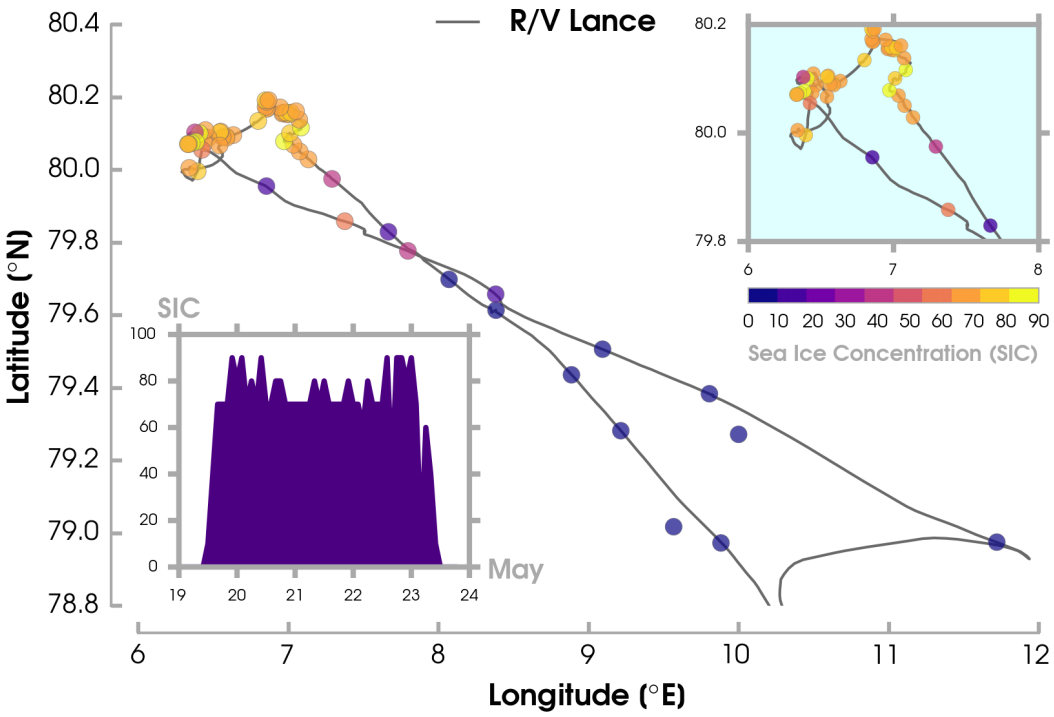

Figure 3. Same as Fig. 1 (different color bar), but only for the R/V *Lance* in situ observations. The ship track is shown in black. The upper right subplot provides a closer view of observations during periods of R/V *Lance* drift. The lower left subplot shows the SIC observations as a continuous time series.

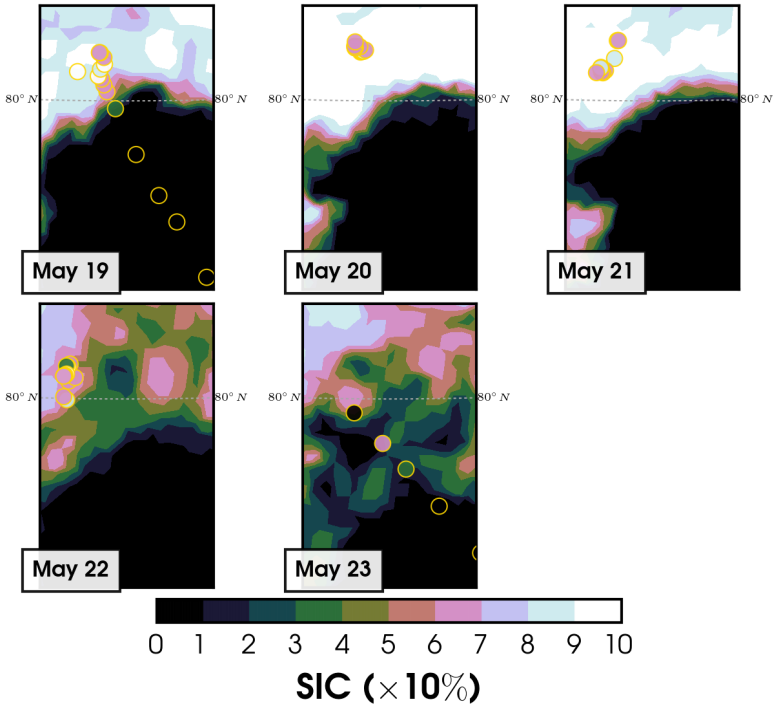

Figure 4. Same as Fig. 1, but separated by days from 19 to 23 May 2017. AMSR2 ASI-3k data also shown for each day.